Effect of transverse mode structure on the far field pattern of metal-metal terahertz quantum cascade lasers

P. Gellie,[1] W. Maineult,[1] A. Andronico,[1] G. Leo,[1] C. Sirtori,[1] S. Barbieri,[1,a)]
Y. Chassagneux,[2] J. R. Coudevylle,[2] R. Colombelli,[2] S. P. Khanna,[3] E. H. Linfield,[3] and A. G. Davies[3]
[1]*Matériaux et Phénomènes Quantiques, Université Paris 7, 10 rue A. Domont et L. Duquet, 75205 Paris, France*
[2]*Institut d'Electronique Fondamentale, Université Paris Sud and CNRS, UMR8622, 91405 Orsay, France*
[3]*School of Electronic and Electrical Engineering, University of Leeds, Leeds LS2 9JT, United Kingdom*

(Received 17 October 2008; accepted 4 November 2008; published online 24 December 2008)

We elucidate the effects of the lateral mode structure on the far field pattern of metal-metal ridge-waveguide terahertz quantum cascade lasers. By introducing a 6-μm-wide metal gap on the top metal contact, we suppress odd-parity lateral modes and drastically modify the far field pattern. Measurements are in good qualitative agreement with full three-dimensional finite-difference-time-domain modeling. Experimental evidence of nonuniform current pumping on the intensity distribution of the guided mode (and hence the far field pattern) is also presented and explained in terms of gain guiding. © *2008 American Institute of Physics*.
[DOI: 10.1063/1.3043795]

I. INTRODUCTION

Metal-metal (MM) waveguides are extensively used for the light confinement in terahertz quantum cascade lasers (QCLs).[1–3] Compared to single-metal waveguides, MM structures allow a stronger mode confinement in both lateral and vertical directions, enabling the fabrication of narrower devices without compromising the overlap factor between the guided mode and the active region, which remains always close to unity. As a result, MM waveguide QCLs have been demonstrated to frequencies as low as 1.2 THz and have yielded record operating temperatures in pulsed and continuous wave mode.[2,4,5]

Experimental far field (FF) patterns from narrow MM waveguide QCLs show a concentric ring-structure centered on the waveguide axis and characterized by a total lack of directionality, which stems from the subwavelength confinement of the guided mode.[6] As long as the lateral dimensions of the waveguide are smaller than the wavelength, such structures can be qualitatively described by approximating the device to a metal wire, standing-wave antenna of length L, with unmatched terminations, and positioned on top of a metallic ground plane.[6–8] However this is a quite extreme situation as the typical waveguide lateral width of terahertz QCLs is several times the wavelength in the material, hindering the application of the wire antenna model for describing FF radiation patterns.

In this letter, we show how the lateral extension and profile of the guided modes affects the FF of QCLs based on MM waveguides. By using (i) MM waveguides with a slightly narrower top metal contact compared to the ridge width and (ii) devices with a few micrometers wide longitudinal gap at the center of the top metal contact, we promote lasing action on lateral modes of zero (TM_{00}) or first order (TM_{01}), respectively, and show their effect on the FF radiation pattern. The experimental results are qualitatively reproduced by three-dimensional (3D) finite difference time domain (FDTD) simulations. Finally, we produce evidence that, thanks to gain guiding effects, the FF emission can be modified by changing the electrical pumping conditions with possible applications to beam steering.

II. EXPERIMENTAL RESULTS AND DISCUSSION

In terahertz QCLs, the active region is sandwiched between two highly doped n^+ GaAs contact layers, essential for the electrical contact. The effect of leaving the doped, top contact layer partially uncovered by the top metallization alters the propagation constant of guided modes and this effect has been exploited already.[9–12] For instance, lasing action on a well defined *longitudinal* mode can be obtained by realizing a periodic array of horizontal apertures (distributed feedback).[9,11] Here, we use longitudinal apertures (along the whole ridge length) on the top metallization of a MM QCL to select effectively laser action on *lateral* modes of different orders. We have performed the experiment on a QCL emitting at $\approx$2.7 THz. The active region—based on a phonon-resonant depopulation scheme, whose details will be reported elsewhere[13]—is 9.9 μm thick and is sandwiched between 75 and 50 nm thick top and bottom contact layers, with a doping concentration of 5×10^{18} cm^{-3}. As shown schematically in the inset of Fig. 1, for a ridge width of 130 μm, lateral mode selection is achieved using two different top metal contact geometries. In both geometries, the top metal contact is narrower than the ridge by approximately 8 μm (4 μm on each side); however in one case we introduced an additional 6-μm-wide longitudinal opening in the

a)Author to whom correspondence should be addressed. Electronic mail: stefano.barbieri@univ-paris-diderot.fr.

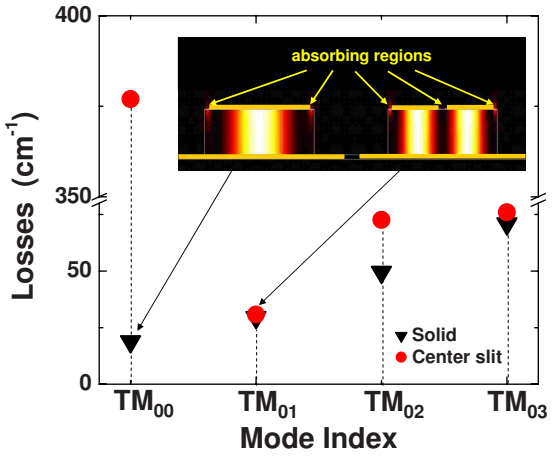

FIG. 1. (Color online) Propagation losses as a function of lateral mode order for a 130-μm-wide ridge with a solid top metal contact (black triangles) and for a ridge with a 6-μm-wide longitudinal slit at the center of the top metal contact (red circles). In both cases, the ridge is 8 μm wider than the metal (4 μm on each side). (Inset) Schematic of the MM waveguides and computed two-dimensional intensity profile of the TM$_{00}$ and TM$_{01}$ modes (dimensions are not to scale). The arrows indicate the regions of the top contact not covered by metal.

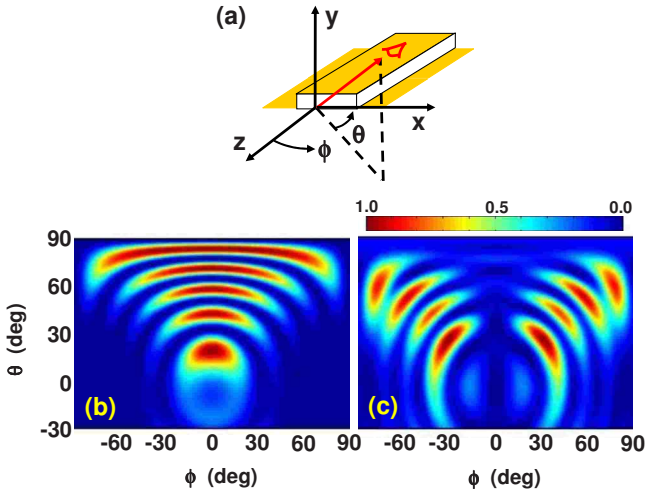

FIG. 2. (Color online) (a) Schematic of the MM waveguide ridge. ϕ and θ are the tangential and azimuthal angles, respectively. The center of the facet is at ϕ=0°, θ=0°. (b) Computed FF radiation pattern using a full 3D FDTD code for a 130×9.9×510 μm^3 ridge with solid top contact. (c) Computed FF for a 130×9.9×490 μm^3 ridge with a 6-μm-wide top central strip (see inset in Fig. 1).

center of the ridge, effectively creating two disconnected metal pads. The effect on the propagation losses of the first four lateral order modes is displayed in the main body of Fig. 1. With a solid top contact, the propagation losses increase monotonically with increasing mode order. As shown in Ref. 12, this results from a progressively higher overlap with the 4-μm-wide lateral contact regions not covered by the top metallization. This trend is modified by the additional central aperture. In this case, while the propagation losses of even modes are unaffected, the losses in the first and third order lateral modes jump to ≈370 and ≈70 cm^{-1}, respectively, owing to a strong overlap of the optical mode with the 6-μm-wide, central, highly doped top contact stripe. Computed losses for the TM$_{00}$ and TM$_{01}$ modes are 19 and 29 cm^{-1} for the solid contact, respectively, and 377 and 31 cm^{-1} after the introduction of the central slit.

In Fig. 2, we show the simulated FF patterns of the devices shown in the inset of Fig. 1. The ridge lengths are 480 and 510 μm for the devices with (panel c) and without (panel b) longitudinal slits, respectively. For the simulation we first computed the electromagnetic field distribution of the eigenmode of interest in the plane perpendicular to the ridge axis using a two-dimensional finite difference frequency domain code. The resulting near field intensity profiles are shown in the inset of Fig. 1. Next we simulated the propagation of an electromagnetic pulse injected at the center of the guide using a 3D FDTD code developed by us. By selectively exciting the appropriate lateral mode, we were able to compute the FFs using the standard near to FF transformation based on the equivalence theorem.[14] All these calculations were performed in the absence of electrical pumping (cold cavity).

The FF distribution mirrors the symmetry of the near fields, yielding a TM$_{01}$ FF-pattern [Fig. 2(c)] characterized by a minimum intensity at ϕ=0°. Both FF patterns are multilobed, and in agreement with the wire-antenna model, we find that the number of lobes increases with increasing cavity length or effective index.[6–8] It is interesting to compare the TM$_{00}$ FF with that in Ref. 6. There, 3.0 THz QCLs with 25-μm-wide MM ridges were used. As confirmed by our simulations (not shown), the effect of narrowing the ridge width below the wavelength in the material is to elongate the lobes until they become full semicircles in the θ>0 hemisphere.

In Fig. 3, we show the measured FF patterns of two MM QCLs *without* (panel a) and *with* (panel b) a longitudinal slit. The ridge dimensions and the emission wavelength are identical to those used for the calculations in Fig. 2. The data were collected by scanning a Golay cell detector with a 2 mm aperture, on a 6 cm radius sphere centered on the laser facet. The FF patterns are in good qualitative agreement with

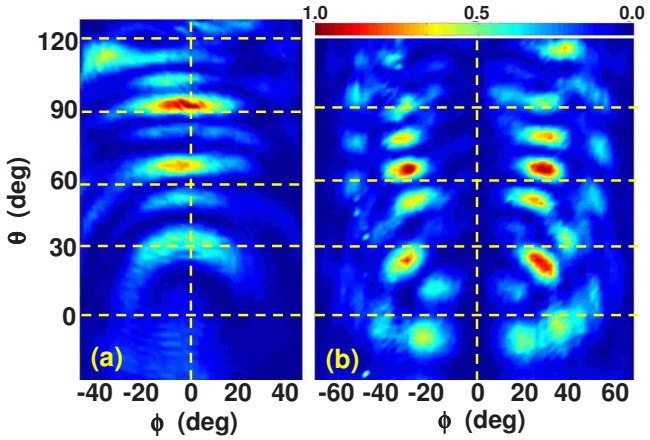

FIG. 3. (Color online) Measured FF radiation patterns for the same ridge dimensions used for the simulations displayed in Fig. 2. (a) Solid top metal. (b) Top metal with central slit. Measurements were performed by scanning a Golay-cell detector on a 6 cm radius sphere. The detector was mounted on a motorized two-axis rotation stage. The lasers were operated at a temperature of 10 K using 1 μs pulses at a 100 kHz repetition rate. The typical current density injected was ≈1 kA/cm^2.

the simulations in Fig. 2. In particular, the introduction of the longitudinal slit modifies the mode symmetry, with the appearance of a clear minimum at $\phi=0°$. This demonstrates that odd-parity modes have been suppressed and validates the effectiveness of our technique for lateral mode selection.

Without entering into a detailed comparison, the main differences between simulated and measured FFs are in (i) the angular span and (ii) the intensity distribution of the high intensity regions. It is likely that the change in the FF patterns is due to a different near field distribution compared to those used for the simulations. Owing to their significantly higher losses, it is safe to assume that no other modes except the TM_{01} are lasing in the device with the central slit (see Fig. 1). On the other hand, TM_{00} and TM_{01} modes could coexist in the device with the solid top contact. However we have found that the measured spectrum of the device is multimode with constant mode spacing. This fact supports the hypothesis that lasing action takes place on purely TM_{00} or TM_{01} modes since otherwise the different lateral effective indices would produce an irregular mode spacing.[15] In this case the FF would result from the coherent superposition of the two modes and would depend on their relative phase. However, the coherence and interference between transverse modes is a complex issue and it is beyond the scope of this article.[16]

Another possible mechanism affecting the 3D spatial distribution of the guided modes is gain guiding induced by an inhomogeneous current distribution in the plane.[17] To investigate further the possibility of gain guiding we deliberately forced a nonuniform current distribution in the device with a central slit by electrically biasing only one of the top metal pads. The effect is shown in Fig. 4 where the measured FFs from a 190-μm-wide, 480-μm-long ridge are presented. When both metal pads are biased [Fig. 4(a)], we recover essentially the same FF symmetry of Fig. 3(b). Instead, the asymmetric bias generates a FF, which is very close to that of Fig. 3(a). To simulate the gain guiding to a first approximation, we have assumed that only the region of the ridge beneath the electrically pumped section is above threshold. In this region we have introduced the effect of gain by artificially modifying the complex refractive index in the active region of the QCL from, $n=3.59+i3.0\times10^{-3}$ to $n=3.59-i3.5\times10^{-2}$, such that the (negative) propagation losses of the guided mode compensate the expected total losses of 29 cm^{-1}.[18] This produces a steplike index profile along the section of the guide, with a change at the midpoint. The resulting near-field profile is displayed in Figs. 4(c) and 4(d), showing a strongly asymmetric intensity distribution, with a mode that is clearly more intense beneath the electrically pumped pad (right). This qualitatively accounts for the change in the FF from Fig. 4(a) to Fig. 4(b), as confirmed by simulations (not shown).

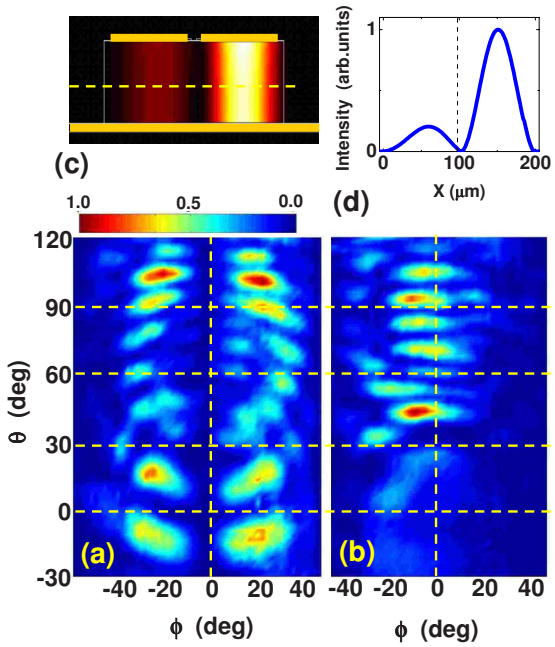

FIG. 4. (Color online) Measured FFs for a $190\times9.9\times490$ μm^3 ridge with top central slit. (a) Both top metal pads are biased [same as for Fig. 3(b)]. (b) Only the right top metal pad is biased. (c) Two-dimensional intensity profile of the guided mode obtained by introducing gain only in the right half of the ridge (dimensions are not to scale). (d) Cross section of the intensity profile of the guided mode. The position of the section is indicated by the dashed line in panel (c).

III. CONCLUSIONS

In conclusion, we have demonstrated lateral mode control in MM terahertz QCLs by suitable patterning of the top metal contact. We have also shown that the FF emission can be modified by changing the electrical pumping conditions, generating gain guiding. We are presently exploring the possibility of exploiting this technique for beam steering.

ACKNOWLEDGMENTS

The device fabrication has been performed at the nanocenter CTU-IEF-Minerve, which was partially funded by the "Conseil Général de l'Essonne." R.C., Y.C., and J.R.C. acknowledge support from the EURYI scheme award (www.esf.org/euryi). Partial financial support from EC projects TERANOVA and POISE, the DGA (Délégation Générale pour l'Armement), and the initiative c-Nano Ile-de-France is also acknowledged. S.P.K., E.H.L., and A.G.D. acknowledge support from EPSRC (U.K.) and HMGCC.

[1] K. Unterrainer, R. Colombelli, C. Gmachl, F. Capasso, H. Y. Hwang, A. M. Sergent, D. L. Sivco, and A. Cho, Appl. Phys. Lett. **80**, 3060 (2002).
[2] B. S. Williams, S. Kumar, Q. Hu, and J. L. Reno, Opt. Express **13**, 3331 (2005).
[3] R. Köhler, A. Tredicucci, F. Beltram, H. E. Beere, E. H. Linfield, A. G. Davies, D. A. Ritchie, R. C. Iotti, and F. Rossi, Nature (London) **417**, 156 (2002).
[4] C. Walther, M. Fischer, G. Scalari, R. Terazzi, N. Hoyler, and J. Faist, Appl. Phys. Lett. **91**, 131122 (2007).
[5] M. A. Belkin, J. A. Fan, S. Hormoz, F. Capasso, S. P. Khanna, M. Lachab, A. G. Davies, and E. H. Linfield, Opt. Express **16**, 3242 (2008).
[6] E. E. Orlova, J. N. Hovenier, T. O. Klaassen, I. Ksalynas, A. J. L. Adam, J. R. Gao, T. M. Klapwijk, B. S. Williams, S. Kumar, Q. Hu, and J. L. Reno, Phys. Rev. Lett. **96**, 173904 (2006).
[7] A. J. L. Adam, I. Ksalynas, J. N. Hovenier, T. O. Klaassen, J. R. Gao, E. E. Orlova, B. S. Williams, S. Kumar, Q. Hu, and J. L. Reno, Appl. Phys. Lett. **88**, 151105 (2006).
[8] C. Balanis, *Antenna Theory*, 3rd ed. (Wiley, New York, 2005).
[9] O. Demichel, L. Mahler, T. Losco, C. Mauro, R. Green, J. Xu, A. Tredicucci, F. Beltram, H. E. Beere, D. A. Ritchie, and V. Tamošiūnas, Opt. Express **14**, 5335 (2006).

[10]Y. Chassagneux, J. Palomo, R. Colombelli, S. Dhillon, C. Sirtori, H. Beere, J. Alton, and D. Ritchie, Appl. Phys. Lett. **90**, 091113 (2007).
[11]S. Kumar, B. S. Williams, Q. Qin, W. M. Lee, Q. Hu, and J. L. Reno, Opt. Express **15**, 113 (2007).
[12]J. A. Fan, M. A. Belkin, F. Capasso, S. P. Khanna, M. Lachab, A. G. Davies, and E. H. Linfield, Appl. Phys. Lett. **92**, 031106 (2008).
[13]Y. Chassagneux, R. Colombelli, W. Maineult, S. Barbieri, S. P. Khanna, E. H. Linfield, and A. G. Davies (unpublished).
[14]A. Taflove and S. C. Hagness, *Computational Electrodynamics. The Finite-Difference Time-Domain Method*, 3rd ed. (Artech House, Boston, 2005).
[15]We compute a difference of ~1% in the effective indices.
[16]W. W. Bewley, J. R. Lindle, C. S. Kim, I. Vurgaftman, J. R. Meyer, A. J. Evans, J. S. Yu, S. Slivken, and M. Razeghi, IEEE J. Quantum Electron. **41**, 833 (2005).
[17]J. Kröll, J. Darmo, K. Unterrainer, S. S. Dhillon, C. Sirtori, X. Marcadet, and M. Calligaro, Appl. Phys. Lett. **91**, 161108 (2007).
[18]The mirror losses are those corresponding to a MM 95-μm-wide ridge, i.e., half the width of the 190 μm ridge used in the experiment. This assumption is justified *a posteriori* by the near field profile in Fig. 4(c).